JGR Biogeosciences

RESEARCH ARTICLE
10.1029/2022JG007183

Key Points:

- Snow cover end date variation explains 12%–90% of spring vegetation phenology variation in 63% of the Pan-Arctic
- In 13% of the Pan-Arctic region, snow cover end date is the dominant factor affecting spring vegetation phenology
- The impact of snow cover end date on spring vegetation phenology varies oppositely with temperature in cold and warm areas

Supporting Information:

Supporting Information may be found in the online version of this article.

Correspondence to:

P. Xiao,
xiaopf@nju.edu.cn

Citation:

Wu, Y., Xiao, P., Zhang, X., Liu, H., Dong, Y., & Feng, L. (2023). Effects of snow cover on spring vegetation phenology vary with temperature gradient across the Pan-Arctic. *Journal of Geophysical Research: Biogeosciences*, *128*, e2022JG007183. https://doi.org/10.1029/2022JG007183

Received 14 SEP 2022
Accepted 24 MAR 2023

Effects of Snow Cover on Spring Vegetation Phenology Vary With Temperature Gradient Across the Pan-Arctic

Youlv Wu[1], Pengfeng Xiao[1,2], Xueliang Zhang[1], Hao Liu[1], Yuanbiao Dong[1], and Lian Feng[3]

[1]Jiangsu Provincial Key Laboratory of Geographic Information Science and Technology, Key Laboratory for Land Satellite Remote Sensing Applications of Ministry of Natural Resources, School of Geography and Ocean Science, Nanjing University, Nanjing, China, [2]Jiangsu Center for Collaborative Innovation in Geographical Information Resource Development and Application, Nanjing, China, [3]School of Environmental Science and Engineering, Southern University of Science and Technology, Shenzhen, China

Abstract Extensive and complex changes in spring vegetation phenology have occurred in the Pan-Arctic over the last several decades. However, the role of snow cover at the start of the growing season (SOS) under different climatic conditions remains unclear. Therefore, we compare the effects of four snow indicators on SOS from 1982 to 2015 based on long-term remote sensing data and found that snow cover end date (SCED) is the main snow indicator affecting SOS, with SOS advancing 0.56 days for each 1-day advance in SCED, explaining 12%–90% of SOS variability in 63% of the Pan-Arctic region. The results also demonstrate that SCED is the dominant factor on SOS in 13% of the Pan-Arctic region and the effects of SCED on SOS vary with temperature gradient rather than precipitation gradient. In cold areas, the positive effect of SCED on SOS diminished with increasing temperature, while in warm areas, the positive effect of SCED on SOS increased with increasing temperature. As the climate warms, the impact of SCED on SOS is expected to weaken in cold areas and increase in warm areas. The findings have crucial implications for understanding future vegetation phenological responses to climate change across the Pan-Arctic.

Plain Language Summary The Pan-Arctic is undergoing dramatic environmental changes. Changes in spring vegetation phenology, one of the most critical climate-induced changes, have not always followed the global advancement trends. The role of changing snow cover in a considerable amount of variation in spring vegetation phenology under various climatic conditions is still not clear. Based on long-term remote sensing datasets, we find that snow cover influenced 63% of Pan-Arctic terrestrial spring vegetation phenology, with a 1-day advance in snowmelt followed by a 0.56-day advance in spring vegetation phenology. The effect of snowmelt on spring vegetation phenology varies by area and is related to the temperature rather than precipitation. There are different modes of the impact of snowmelt on spring vegetation phenology in cold and warm areas. The impact of early snowmelt on spring vegetation phenology is expected to diminish in cold areas and increase in warm areas as the climate warms across the Pan-Arctic. Our results contribute to a better understanding of the future vegetation status of the Pan-Arctic ecosystem in the context of climate change.

1. Introduction

Changes in vegetation phenology in spring, particularly the start of the growing season (SOS), are critical climate-induced changes (Piao et al., 2019; Richardson et al., 2013) that can alter the length of the vegetation growing season and influence the carbon, water, and energy fluxes between the terrestrial ecosystems and the atmosphere (Keenan et al., 2014; Kim et al., 2018; Linderholm, 2006; Penuelas et al., 2009). Spring temperature is an environmental variable widely used to explain variation in spring vegetation phenology (de Beurs & Henebry, 2005, 2008; Panchen & Gorelick, 2017; Prevéy et al., 2017). Despite the global trend of advancing SOS since the early 1980s due to increasing temperatures (Piao et al., 2019), changes in SOS in the Pan-Arctic region, where temperatures rise sharply, do not always follow these trends. Instead, the SOS in some areas advances while it delays or remains unchanged in others, reflecting substantial complex variation (H. Zeng et al., 2011; Zheng et al., 2020). Moreover, changing snow cover complicates the relation between temperature and spring vegetation phenology and has been proven to play an important role in a considerable amount of the complex variation in spring vegetation phenology (Bjorkman et al., 2015; Buus-Hinkler et al., 2006; Legault & Cusa, 2015; Semenchuk et al., 2016; Wipf & Rixen, 2010).

Snow cover affects SOS by altering the soil water, heat, and nutrient cycles (Freppaz et al., 2008; Harpold & Molotch, 2015; Rixen et al., 2008). For instance, snow layers protect plants from frost damage, desiccation, and photoinhibition (Lundell et al., 2010; Mølgaard & Christensen, 2010; Sherwood et al., 2017) and provide soil moisture and nutrients for plant growth (Harpold & Molotch, 2015; Rixen et al., 2008). Thin layers of snow that melt quickly can increase the probability of frost formation and reduce the soil temperature, consequently, limiting plant growth (Bokhorst et al., 2011; Wipf et al., 2006). The importance of snow cover end date (SCED) on the SOS has been demonstrated by many field-based plot-scale studies (Assmann et al., 2019; Cooper et al., 2011; Iler et al., 2017; Wipf, 2010; Zheng et al., 2022). Snow cover onset date (SCOD), snow cover duration (SCD), and snow water equivalent (SWE) can also affect the SOS (Borner et al., 2008; Jonas et al., 2008; K. Wang et al., 2015; Westergaard-Nielsen et al., 2017; Xie et al., 2018). Different snow indicators are interrelated and relatively partially independent. Still, few studies in the Pan-Arctic have clarified the impact of snow cover on SOS when different snow indicators are considered comprehensively. Therefore, the effect of snow cover as a phenological driver of SOS is not fully understood.

Previous studies based on experimental or observational data have suggested that the impact of snow cover on the SOS varies with local hydrothermal conditions and topographic conditions (Kelsey et al., 2021; Paudel & Andersen, 2012; S. Wang et al., 2017; X. Wang et al., 2017; X. Wang et al., 2018). X. Wang et al. (2018) found that most regions of the Tibetan Plateau exhibited a positive correlation between SOS and snowmelt timing, while the opposite response was observed in warmer but drier areas. Moreover, Paudel and Andersen (2012) reported that changes in snow cover and precipitation patterns play a more important role in rangeland vegetation dynamics in snow-fed, drier areas. The Pan-Arctic is currently experiencing a significant increase in temperature, which is accompanied by alterations in snow cover and various other climatic conditions (Meredith et al., 2019). Previous studies have focused on localized sites or specific species to explore the associations among climatic conditions, snow cover, and vegetation phenology in the Pan-Arctic (Oberbauer et al., 2013; Wheeler et al., 2015; Zheng et al., 2022). For instance, Oberbauer et al. (2013) used species-level phenological event data from 12 sites in International Tundra Experiment (ITEX) and found that dry sites generally have light snow cover and warmer soils, thus vegetation emerges from the snow earlier than in wet and moist sites. Recently, based on multiple ground observations and remote sensing products in Alaska and part of Yukon, Zheng et al. (2022) discovered that SOS is less sensitive to SOM in Temperate Coastal with suitable temperatures and abundant precipitation, and more sensitive to SOM in Bering Taiga located in moist polar climates with relatively abundant precipitation. However, past studies with limited data and restricted perspectives have limited our understanding of the response of SOS to snow cover under different climatic conditions across the Pan-Arctic.

This study comprehensively evaluates the influence of snow cover changes on the SOS across the Pan-Arctic (>60°N latitude) using long-term remote sensing data. Specifically, we aim to (a) quantify the effect and identify the importance of snow cover on the SOS; and (b) investigate the impacts of snow cover on the SOS under different climatic conditions. Therefore, the corresponding results will further enhance our understanding of the effects of snow cover on the SOS at the circumpolar scale in the context of climate change. Additionally, the findings will improve the predictions of the response of vegetation to changing plant growth conditions across the Pan-Arctic.

2. Materials and Methods

2.1. Observational Data Sets

The Pan-Arctic region (Northern Hemisphere with latitudes more than 60°N) is selected as the study area (Brown et al., 2010; Luus et al., 2013). Daily SWE observations for 1980–2018 at a spatial resolution of 25 km are obtained from the GlobSnow SWE product, which is derived from a combination of ground-based snow depth observations and satellite-based passive microwave radiometer data in an assimilation scheme (Luojus et al., 2020; Pulliainen, 2006; Takala et al., 2011). The GlobSnow SWE product is selected because it provides a more realistic observation-based estimate of SWE over the Pan-Arctic than previous passive microwave algorithms (AMAP, 2017; Pulliainen et al., 2020).

The satellite-derived normalized difference vegetation index (NDVI) is a proxy for vegetation greenness and photosynthetic activity (Myneni et al., 1995) and is commonly used to interpret the SOS by extracting land surface phenology (Buitenwerf et al., 2015; Cong et al., 2013; de Beurs & Henebry, 2010). We use the GIMMS NDVI3g data set developed by NASA and derived from AVHRR sensors at a spatial resolution of 1°/12° and a

temporal resolution of 15 days for 1981–2015. Further, the GIMMS NDVI3g data set is corrected for calibration, solar geometry, heavy aerosols, clouds, other effects unrelated to vegetation change, and discontinuities in the GIMMS NDVI data set north of 72°N (Pinzon & Tucker, 2014). As the longest continuous data set of global vegetation activities, GIMMS NDVI3g is currently the most suitable choice for long-term vegetation trend analysis (Tian et al., 2015).

Daily temperature, precipitation, and radiation data are from the ECMWF ERA-5 hourly data set, a climate reanalysis data set that provides a consistent view of the evolution of climate variables over decades from 1979 to the present at a spatial resolution of 0.25° × 0.25° (Hersbach et al., 2020). ERA-5 performs well in terms of temperature, precipitation, and radiation in the Arctic compared to several other common reanalyses or ground-based and satellite observations (Barrett et al., 2020; Graham et al., 2019; Trolliet et al., 2018). In addition, the Climate Change Initiative Land Cover (CCI LC) data set with 300 m spatial resolution from 1992 to 2015 classifies land cover into 22 types based on the Land Cover Classification System (LCCS) approach (ESA, 2017). It is a suitable data set for analyzing Pan-Arctic vegetation with an appropriate classification system (Bartsch et al., 2016) and relatively high accuracy for classifying forest, shrubs, and sparse vegetation (Li et al., 2019). We retain pixels with unchanged land cover types, select the main vegetation types and reclassify them as evergreen needleleaf forest (ENF), deciduous needleleaf forest (DNF), mixed forest (MF), mosaic vegetation cover (MV), shrubland (SH), grassland (GL), sparse vegetation (SV), and wetland (WET).

Since the above-mentioned datasets comprise different time series, we limit the analysis to 1982–2015 to correspond to the NDVI series. Furthermore, all datasets are aggregated to a spatial resolution of 25 km × 25 km using the nearest neighbor resampling technique to match the SWE data set resolution. Although some recent studies suggested a possible deceleration or reversal in the trend of advancing SOS since the 2000s in some areas (Park et al., 2018), we conduct additional analyses for two different periods (1982–1997 and 1998–2015) to explore the effect of snow cover on SOS in Supporting Information (Figures S1–S10 in Supporting Information S1). Notably, our key findings remain consistent across the different periods studied.

2.2. Determination of Snow Indicators and SOS

Based on the seasonal cycle of snow cover over the Pan-Arctic, we define the period from 1 August to 31 July of the following year as a hydrological year to derive the snow indicators (Mudryk et al., 2020). SCOD is defined as the first date of the first five continuous snow cover days, SCED is defined as the last date of the last five continuous snow cover days (S. Wang et al., 2017; X. Wang et al., 2017), and SCD is defined as the number of snow cover days between the snow cover start date and the SCED during a hydrological year (Zhong et al., 2021). Further, snow accumulation (SWE_{max}) is defined as the maximum value of the snow water equivalent in a hydrological year.

Snowmelt would increase spring NDVI, which can confound the derivation of SOS (Delbart et al., 2006; Jin & Eklundh, 2014). Before SOS extraction, we thus replace the snow-contaminated NDVI values with the mean value of the uncontaminated non-growing season NDVI values based on the snow flag provided by the GIMMS NDVI3g quality field for each pixel (Shen et al., 2014). After removing snow contamination, the Savizky-Golay filter is applied to reduce the noise (X. Wang et al., 2019). Areas with $NDVI_{max}$ <0.1 are considered non-vegetated areas and are excluded from SOS extraction. Due to the weak seasonal variation of some evergreen vegetation, there is large uncertainty in remote sensing to extract phenological information about evergreen vegetation (Wu et al., 2014). Therefore, we exclude the pixels whose difference between the multi-year mean of NDVI in the growing season and the multi-year mean of NDVI in the non-growing season is less than 0.1, to reduce the uncertainty of phenological extraction.

The SOS extraction method includes two steps (J. Zeng et al., 2020). The first step is the reconstruction of the daily NDVI time series using a data filter function. The double logistic function, as shown in Equation 1, is used to fit the NDVI time-series data set in this study, which is more suitable than other algorithms at high latitudes with persistent snow cover (Beck et al., 2006).

$$y(t) = a + b\left(\frac{1}{1+e^{c(t-d)}} + \frac{1}{1+e^{e(t-f)}}\right) \quad (1)$$

where a is the initial background NDVI value; b is the maximum NDVI value; t is the time in days; $y(t)$ is the NDVI value at time t; and c, d, e, and f are parameters that need to be set.

The second step is the determination of the SOS from the NDVI time series. We select two commonly used methods (inflection point detection method and dynamic threshold method) to extract the SOS (J. Wang et al., 2022; Wu et al., 2021). The former method determines the inflection point in the reconstructed NDVI time-series curve. We determine the date corresponding to the maximum value of the first-order derivative of the fitted curve as the SOS (White et al., 1997). The second method, which compares the smoothed NDVI time series with a fixed percentage of the annual maximum, determines the date, corresponding to the first day of the season in which the threshold of $Ratio_{day}$ is exceeded, as the SOS.

$$Ratio_{day} = \frac{NDVI_{day} - NDVI_{min}}{NDVI_{max} - NDVI_{min}} \quad (2)$$

where $Ratio_{day}$ is the ratio of the annual amplitude of NDVI on a given day, and the threshold of $Ratio_{day}$ is set as 0.5; $NDVI_{day}$ is the fitted NDVI on a given day; $NDVI_{max}$ and $NDVI_{min}$ are the maximum and minimum NDVI each year, respectively (Descals et al., 2020). We further screen the valid dates for SOS within 1–200 day of year (DOY) and retain the pixels for which SOS could be extracted for all 34 years. To reduce the SOS uncertainty due to the differences between the two methods, we apply both methods together and average the results to determine the SOS.

2.3. Statistical Analysis

We first calculate the annual means of the four snow indicators (SCOD, SCED, SCD, and SWE_{max}) and SOS for the period 1982–2015 and estimate their trends using the Theil-Sen median slope estimator and a modified Mann-Kendall test for time-autocorrelated data (Hamed & Rao, 1998). To investigate the relation between snow and SOS, we apply a partial correlation analysis per pixel to remove the impacts of pre-season mean temperature, total precipitation, and total radiation. Pre-season length (range: 15–120 days, in 15-day steps) is defined as the period before SOS when climatic factors show the highest absolute value of partial correlation coefficient with the determined SOS date.

To find the most representative snow indicator from the four snow indicators, we use simple linear regression to evaluate the between-year effects of the four snow indicators on SOS, and calculate the annual mean SOS of different snow indicator ranges and use simple linear regression to calculate the between-site effects of the four snow indicators on the SOS. Because of the correlation between the snow indicators, stepwise regression is used to eliminate interference to identify the main snow indicators affecting SOS per pixel. Furthermore, using the representative snow indicator, we determine the contribution of snow cover to SOS based on the determination coefficients per pixel. Additionally, to assess the relative importance of snow cover, we compare the values of partial correlation coefficients of snow cover and climate indicators with SOS, and the indicator with the largest partial correlation coefficient is the relatively most important indicator affecting SOS.

Finally, to investigate the effects of snow cover on SOS under various climatic conditions, we divide the study area into different climatic zones at temperature intervals of 1°C and precipitation intervals of 50 mm; and for each zone, we calculate the mean value of the partial correlation coefficient for pixels with significant partial correlation ($p < 0.05$) between snow and SOS, and target the analysis for different vegetation types. We use the piecewise linear regression (Equation 3) to further determine if the temperature and precipitation affect the relations between SOS and snow cover (X. Wang et al., 2011).

$$y = \begin{cases} \beta_0 + \beta_1 t + \varepsilon & t \le \alpha \\ \beta_0 + \beta_1 t + \beta_2 (t - \alpha) + \varepsilon & t > \alpha \end{cases} \quad (3)$$

where t is annual mean temperature or annual total precipitation; y is the correlation coefficient between SOS and snow cover; α is the turning point of the effect of annual mean temperature or annual total precipitation and is determined by least square error methods; β_0, β_1, and β_2 are regression coefficients; and ε is the residual of the fit. The effect of annual mean temperature or annual total precipitation is β_1 before the turning point, $\beta_1 + \beta_2$ after it. To avoid having few data points, a minimum of five data points is required to participate in the linear regression. Data points with less than 10 pixels are excluded from the linear regression. We use a t-test to assess the necessity of introducing a turning point, and a p-value <0.05 is considered significant.

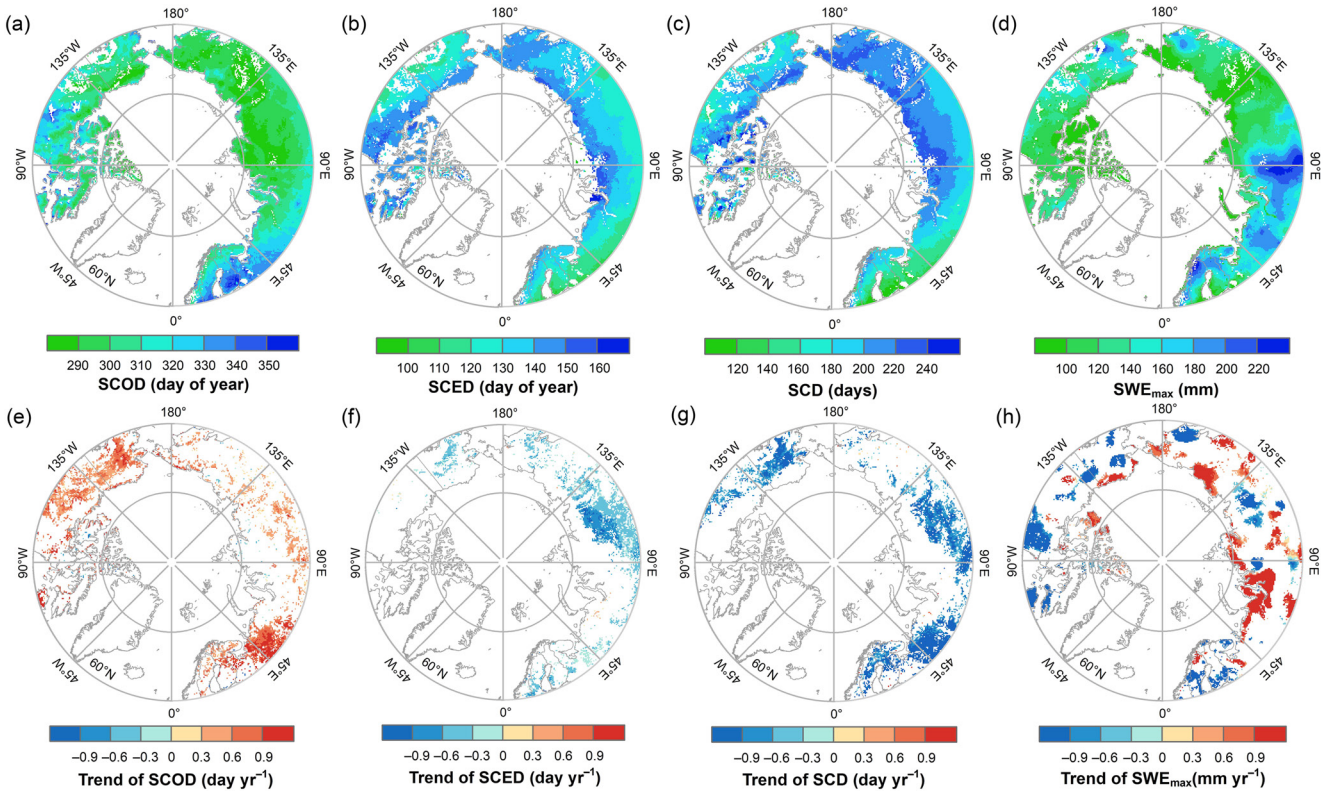

Figure 1. Spatial distributions of the annual mean and trends of snow cover onset date, snow cover end date, snow cover duration, and SWE_{max} during 1982–2015 across the Pan-Arctic (only the pixels with $p < 0.05$ retained).

3. Results

3.1. Spatiotemporal Dynamics of Snow Cover and SOS

The spatiotemporal variability of the snow indicators (SCOD, SCED, SCD, and SWE_{max}) and SOS during 1982–2015 across the Pan-Arctic are illustrated in Figures 1 and 2.

The annual means of SCED and SCD showed similar spatial patterns and exhibited a trend of delay or extension with increasing latitude, respectively, with the earliest SCED area (DOY < 110) and the shortest SCD area (days < 140) observed in Europe near 60°N latitude (Figures 1b and 1c). The SCED (25.7% of the area) and SCD (37.0% of the area) decreased at rates of -0.46 ± 0.21 day yr^{-1} and -0.95 ± 0.37 day yr^{-1}, respectively (Table 1). In contrast, the annual mean of SCOD advanced with increasing latitude, with the latest SCOD area (DOY > 340) observed in Europe near 60°N latitude (Figure 1a), and SCOD significantly delayed in 23.5% of the Pan-Arctic. The SWE_{max} spatial pattern differed, with high SWE_{max} values concentrated in Europe and Central Siberia, with the maximum value reaching 342 mm (Figure 1d and Table 1). The spatial distribution of the SWE trend appeared in clusters, with the most significant increasing and decreasing trends in Western Siberia and eastern Canada, respectively (Figure 1h).

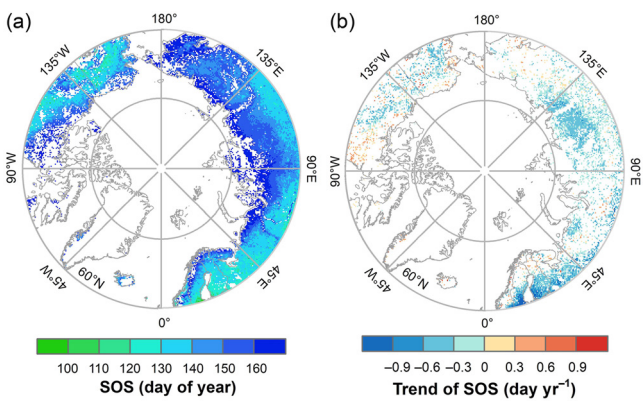

Figure 2. Spatial distributions of the annual mean and trend of start of the growing season during 1982–2015 across the Pan-Arctic (only the pixels with $p < 0.05$ retained).

The annual mean SOS delayed as the latitude increased, with the earliest SOS area (DOY < 120) occurring in Europe and Alaska near 60° N latitude (Figure 2a). SOS was significantly advanced (28.7% of the area), mainly in Europe and Central Siberia, at a rate of -0.37 ± 0.19 day yr^{-1}, while it was considerably delayed (4.9% of the area) in parts of Canada and Alaska at a rate of 0.32 ± 0.17 day yr^{-1} (Figure 2b and Table 1). In general, the spatial

Table 1
Maximum and Minimum of Multi-Year Averaged Snow and Vegetation Indicators and the Proportion and Rate of Positive and Negative Changes in These Indicators During 1982–2015

Snow and vegetation indicator	Minimum (DOY/days/mm)	Maximum (DOY/days/mm)	Positive change proportion	Positive change rate (day yr^{-1}/mm yr^{-1})	Negative change proportion	Negative change rate (day yr^{-1}/mm yr^{-1})
SCOD	277	363	23.5%	0.67 ± 0.30	0.6%	-0.58 ± 0.41
SCED	74	161	0.3%	0.33 ± 0.24	25.7%	-0.46 ± 0.21
SCD	15	242	0.3%	1.02 ± 1.25	37.0%	-0.95 ± 0.37
SWE_{max}	0	342	16.0%	1.19 ± 0.67	14.4	-1.31 ± 0.60
SOS	90	181	4.9%	0.32 ± 0.17	28.7%	-0.37 ± 0.19

patterns of the annual mean of snow cover and SOS are similar, and the five variables vary according to the gradients of climatic and topographical conditions.

3.2. Effects of Snow Cover Change on SOS Variability

To understand the relation between snow cover change and SOS variability, we calculate the partial correlation coefficients between the snow indicators and SOS (Figures 3a–3d). Our analysis revealed that SOS demonstrated the strong positive correlation with SCED and SCD, mainly in Central Siberia and Western Siberia, as well as in regions of Alaska, western Canada, and Europe. Moreover, SOS exhibited positive correlations with SWE_{max}, mainly in western and Eastern Siberia, as well as in Alaska. Nevertheless, our findings also revealed a negative correlation between SOS and SCOD in parts of Central Siberia, Europe, and western Canada.

The simple regression results showed that the SOS was advanced by 0.56/0.18 days with SCED advancing/SCD shortening by 1 day for different years, while the interannual variations of SCOD and SWE_{max} had no significant effect on SOS (Figures 3e–3h). Moreover, for different sites, the SOS was advanced by 0.84/0.29/0.04 day for sites with SCED advancing/SCD shortening by 1 day or SWE_{max} increasing by 1 mm (Figures 3j–3l), while in contrast, SOS was delayed by 0.35 day with each 1-day advancement of SCOD (Figure 3i). SCED had the strongest between-sites and between-years effects on SOS compared to other snow indicators. In addition, the determination coefficients (R^2) between the snow indicators and SOS for different sites were greater than that for different years, which indicates that the between-sites effect of snow on SOS is more significant than the between-years effect. After excluding the correlation between snow indicators, we found that SCED was the most significant snow indicator affecting SOS in most areas and has stronger positive effects in Europe and Western Siberia than in other areas. In contrast, SCOD, SCD, and SWE_{max} had minor impacts on SOS in most areas (Figures 3m–3p). Overall, SCED is a representative snow indicator in the Pan-Arctic region and we used SCED as a proxy for snow cover in subsequent analyses.

To further determine the impact and importance of snow cover on SOS, we quantified the effect of SCED on SOS across the Pan-Arctic. SCED variability explained 12%–90% of the variation in SOS across 63% of the Pan-Arctic, particularly in Western Siberia, Central Siberia, and western Canada (Figure 4a). In 13% of the Pan-Arctic, specifically in Western Siberia and Europe, SCED was identified as the primary factor affecting SOS. On a larger scale, the temperature was found to be the dominant factor, accounting for 45% of the Pan-Arctic and exhibiting a strong correlation with SOS in Central Siberia, northern Europe, Alaska, and western Canada (Figure 4b). Precipitation and radiation played minor roles in only a few areas.

3.3. Effects of SCED on SOS Under Different Climatic Conditions

Because the influence of snow cover dynamics on the SOS is highly dependent on the climatic background and the Pan-Arctic region has a large spatial variation in climatic conditions, we further examined the influence of SCED changes on the SOS under the influence of climatic conditions.

SOS was mainly positively correlated with SCED, and their correlation coefficient varied with the climatic gradient and was significantly ($p < 0.05$) influenced by temperature rather than precipitation (Figure 5a). The

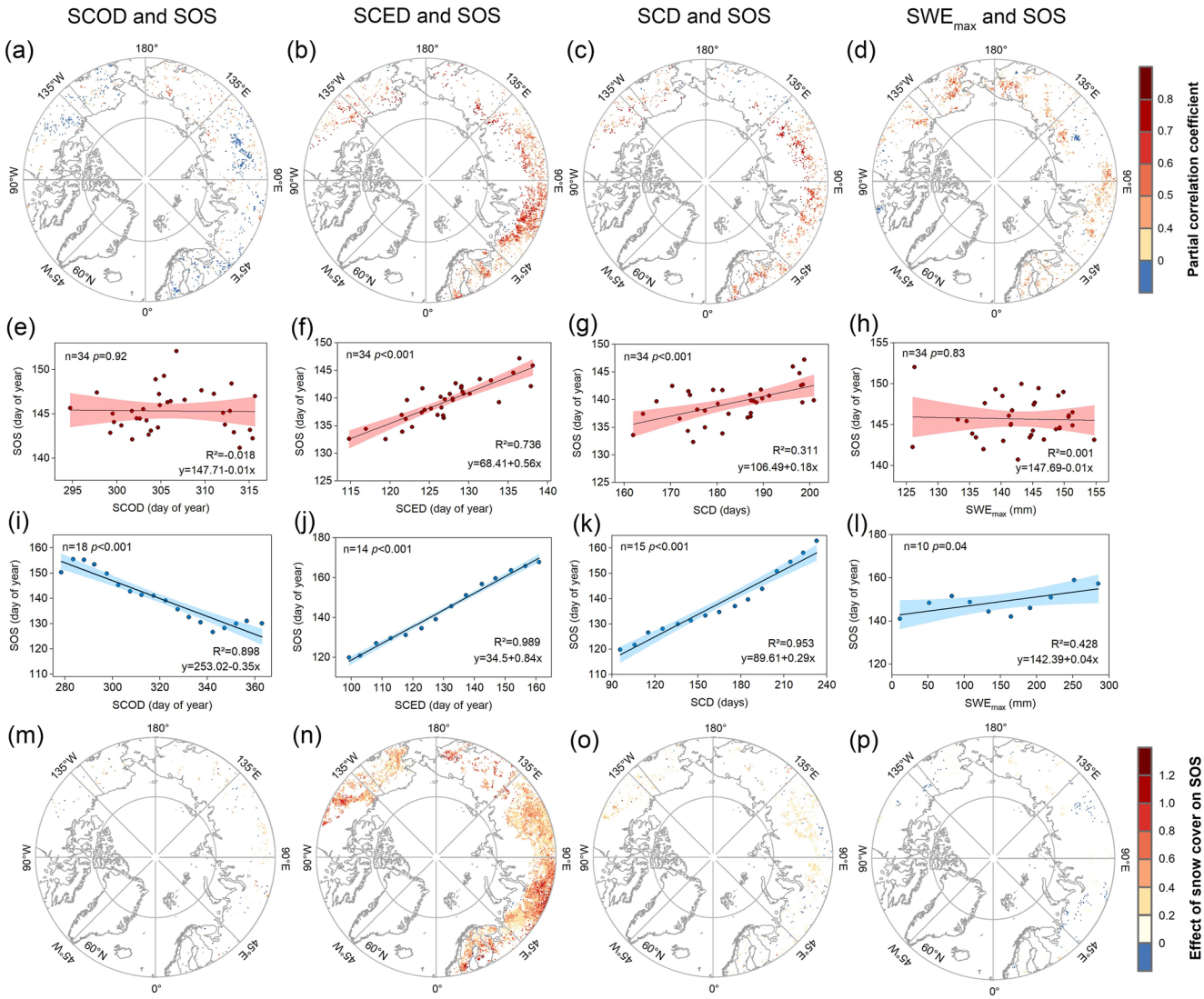

Figure 3. Relations between snow cover and start of the growing season (SOS). (a–d) are spatial patterns of the partial correlations between SOS and the snow indicators (only the pixels with $p < 0.05$ retained). (e–h) are between-year effects of snow indicators on the SOS. The data points represent the snow indicators and SOS mean values for each year. (i–l) are between-site effects of snow indicators on the SOS. The data points represent SOS multi-year means for multi-year mean intervals of different snow indicators. In (e–l), the solid line indicates a significant trend, the shaded area represents the 95% confidence interval, *n* indicates the number of data points, R^2 represents the determination coefficient of the linear fit, and the *p*-value indicates the significance level. (m–p) are spatial patterns of the main snow indicators affecting the SOS obtained by stepwise regression.

annual mean temperature in most study areas was below 1°C. Additionally, higher temperatures weakened the positive correlation between SCED and SOS in these areas, meaning that the coldest areas usually had the largest correlation coefficients for the same precipitation conditions. However, in warmer areas with an annual mean temperature greater than 1°C, in Europe, the positive correlation between SCED and SOS strengthened with increasing temperature, meaning that the warmest areas usually had the largest correlation coefficients for the same precipitation conditions.

Among the pixels where SCED and SOS were significantly correlated, the response of SOS to SCED varied among the eight vegetation types (Figures 5b and 6). The correlations between SCED and SOS were strong for GL, SV, and WET with partial correlation coefficients of 0.58, 0.58, and 0.52, respectively, while for ENF, DNF, MV, and MF, the correlations between SCED and SOS were weaker with partial correlation coefficients of 0.49, 0.49, 0.49, and 0.47. The lowest correlation coefficient between SCED and SOS was found in the SH, at 0.38. ENF accounted for the largest proportion (35% of the area) and was widely distributed in areas with an annual

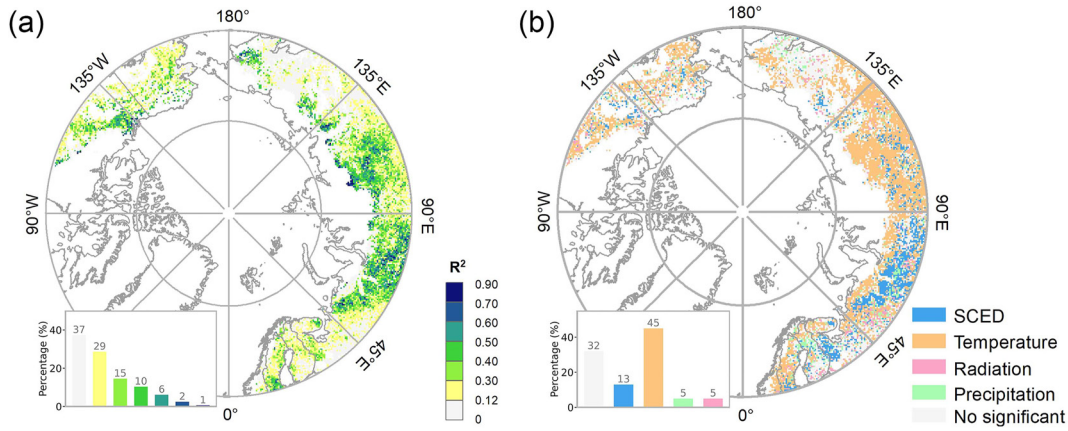

Figure 4. Effect and importance of snow cover end date (SCED) on start of the growing season (SOS). (a) Spatial distribution of determination coefficients (R^2) of the linear regression of SOS and SCED. (b) Spatial distribution of the relatively most important indicators affecting SOS. The bar charts illustrate the proportion of different determination coefficient intervals and different indicators. The gray area represents the non-significant area ($p \geq 0.05$).

mean temperature greater than −9°C, mainly in northern Canada, Europe, and Western Siberia. DNF (26% of the area) occurred in areas with annual mean temperatures less than −1°C, mainly in Central Siberia. WET (16% of the area) was concentrated in Western Siberia, while MV (6% of the area) was sporadically distributed in the study area. SH (5% of the area), MV (4% of the area), and GL (3% of the area) were found in the drier and colder areas, while MF (5% of the area) was distributed in wetter and hotter areas, near 60°N in Europe.

4. Discussions

4.1. Importance of Snow Cover on SOS Across the Pan-Arctic

Significant correlations between SOS and different snow indicators can be observed in different areas (Figure 3), consistent with previous studies that examined the effect of each snow indicator on SOS separately (Borner et al., 2008; Cooper et al., 2011; Westergaard-Nielsen et al., 2017). Snow cover variability can explain SOS variability to some extent across the Pan-Arctic, and is even relatively most dominant influence in some areas, and it

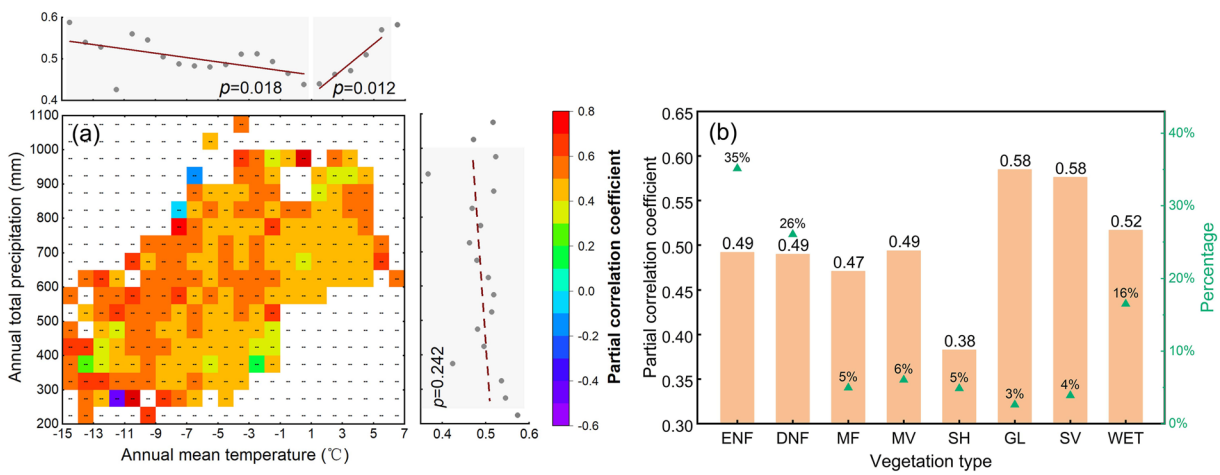

Figure 5. Variations in the partial correlation coefficients between snow cover end date (SCED) and start of the growing season (SOS) along (a) temperature and precipitation gradient and (b) vegetation type over the Pan-Arctic. In (a), each zone represents the mean value of the significant partial correlation coefficients between the SCED and SOS in a specific interval of annual mean temperature and annual total precipitation. The annual mean temperature and annual total precipitation gradients are binned every 1°C and 50 mm, respectively; each dot represents a bin. The solid and dashed lines indicate significant and insignificant trends, respectively. The p values represent the significance. In (b), each bar and triangle represent the partial correlation coefficient between SCED and SOS and the area percentage for each vegetation type, respectively.

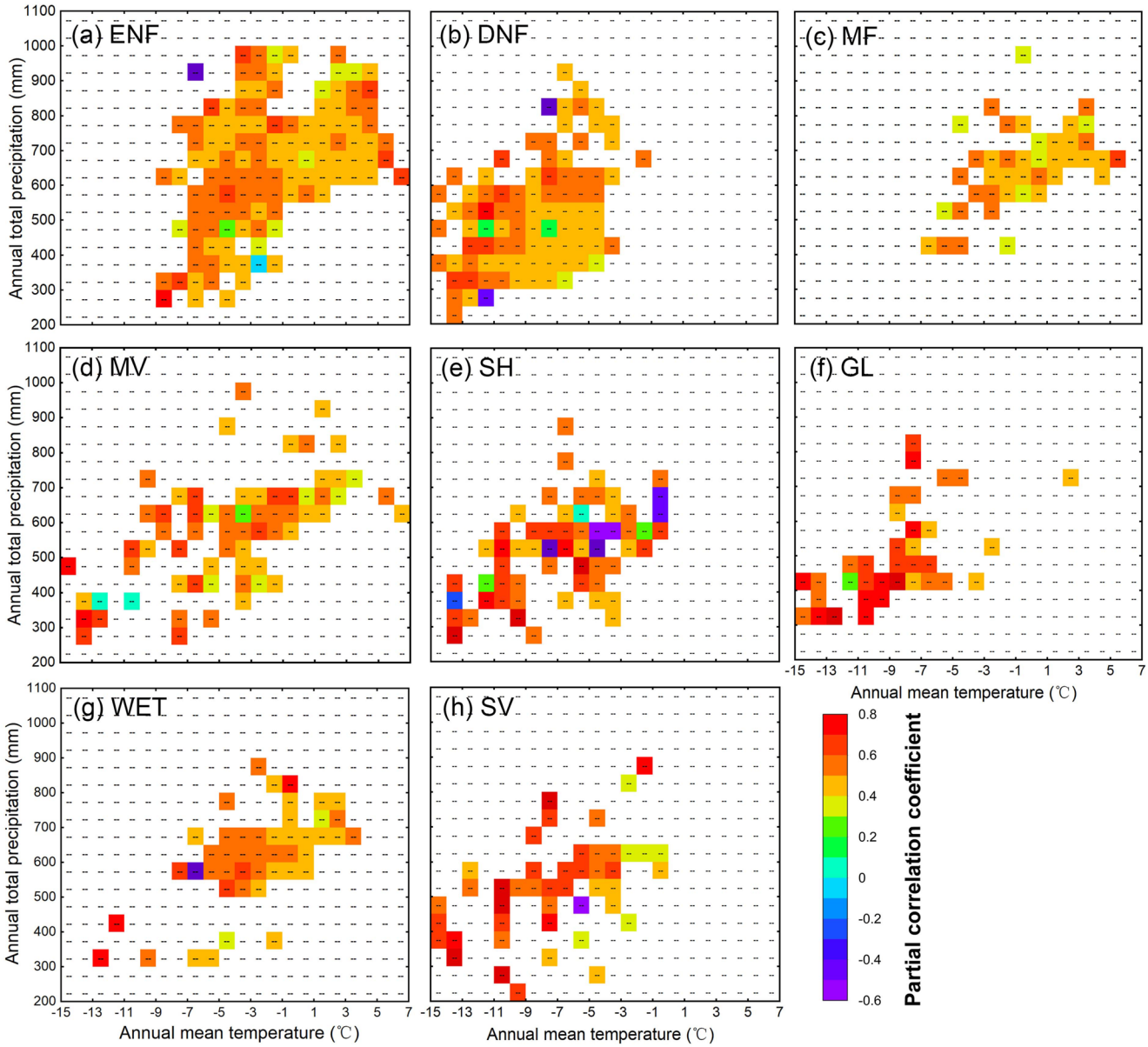

Figure 6. Relations between snow cover end date (SCED) and start of the growing season (SOS) across different climatic conditions for the eight main vegetation types over the Pan-Arctic. The annual mean temperature and annual total precipitation gradients are binned every 1°C and 50 mm, respectively. Each zone represents the mean value of the significant partial correlation coefficients between the SCED and SOS in a specific climatic interval.

is even the most dominant influence in some areas (Figures 3 and 4). On analyzing the influence of snow cover changes on SOS for different years or sites, we found that between-year effects are generally less pronounced than between-site effects (Figure 3). According to a 10-year study of the Alps by Jonas et al. (2008), between-year effects represent short-term responses of plant communities to changing climate, with less change because the vegetation cannot adapt quickly (Totland & Alatalo, 2002), while between-site effects represent long-term responses after vegetation adaptation (Walther et al., 2005). These findings, also observed at the circumpolar scale in this study, suggest that snow cover plays an important role in short- and long-term vegetation change and indicate possible future changes in the SOS under current climate change conditions.

After considering the correlations among snow indicators, we found that SCED is the most critical snow indicator affecting SOS across the Pan-Arctic (Figure 3), which agrees with previous studies that have highlighted the importance of SCED (Assmann et al., 2019; Bjorkman et al., 2015; Wipf, 2010; Zheng et al., 2022). We observed

a significant positive correlation between SCED and SOS, implying that changes in SOS coincide with changes in the timing of snowmelt, as snow no longer blocks incident photosynthetically active radiation (PAR), which stimulates plant development (Buus-Hinkler et al., 2006). The insulation provided by snow can protect vegetation from low-temperature frosts, and low vegetation can increase soil temperature, potentially playing a more important role than air temperature (Zheng et al., 2022). However, it may also cause a lack of chilling requirements for specific species, but colder temperatures in the Pan-Arctic can usually meet the requirements in early fall. Moreover, increased soil moisture and nutrients after snowmelt can promote vegetation growth (Harpold & Molotch, 2015; Rixen et al., 2008).

There was significant spatial heterogeneity in the effects of SCED on SOS (Figure 3), suggesting the influence of other factors on SOS. Various environmental constraints, such as temperature (Shimono & Kudo, 2005), precipitation (Jonas et al., 2008), soil nutrients (Weintraub & Schimel, 2003), photoperiod limitation (Basler & Körner, 2012), and permafrost (Iwata et al., 2010), may inhibit plants from utilizing snowmelt. Additionally, vegetation differences can also affect the SCED–SOS relation (Yu et al., 2013). In summary, our results highlight the importance of SCED for predicting tundra vegetation phenology in spring. At the circumpolar scale, we demonstrate the importance of SCED for SOS over other snow indicators based on long-term data and identify the spatial extent of the effects of SCED on SOS.

4.2. Effects of SCED on SOS Influenced by Temperature

The importance of temperature for SOS is observed in most of the study areas (Figure 4b), implying that Pan-Arctic plant growth is limited by temperature, in agreement with previous knowledge (Ernakovich et al., 2014; Kelsey et al., 2021). However, no significant effect of precipitation on SOS is observed (Figure 4b), which is consistent with the previous finding that areas above 50° N are "vegetation water surplus regions" or areas where vegetation growth is not affected by water by Jiao et al. (2021), meaning that vegetation growth in these areas is not limited by water shortage.

In the cold areas with an annual mean temperature below 1°C, a higher annual mean temperature weakens the positive correlation between SCED and SOS (Figure 5a), which means that the SCED shows the most significant correlation with SOS in the coldest areas. On the one hand, the warmer the areas, the lower the correlation coefficient between SCED and SOS for most vegetation types (Figure 7b), this may be due to the higher the annual mean temperature, the earlier the snow melts, the less effective the insulation of snow cover and the greater the frost risks to vegetation. This mechanism has been observed in some field experiments (Groffman et al., 2001; Sherwood et al., 2017); on the other hand, in colder areas, strong correlations between SCED and SOS are observed for WET, SV, GL, SH, and MV (Figure 7a). Since snow is more likely to cover low vegetation, such as grassland, and shrubland, the insulation of snow can isolate low temperatures, leading to a more pronounced effect of snow cover on low vegetation (Freppaz et al., 2008; Zheng et al., 2022). The warmer the area, the lower the proportion of low vegetation where SCED and SOS are strongly correlated decreases, while MF, MV, ENF, and WET, with smaller correlation coefficients, dominate (Figure 7). In summary, the colder the area, the stronger the positive effect of SCED on SOS in these cold areas.

In warm areas with mean annual temperatures greater than 1°C and total annual precipitation greater than 600 mm, mainly in Europe, a higher annual mean temperature enhances the positive correlation between SCED and SOS (Figure 5a). The warmer the area, the more ENF, MF, and MV dominate, and the correlations between SCED and SOS of different types of vegetation all increase with increasing temperature (Figure 7). In tall vegetation communities such as woodlands and tall scrub, canopy snowmelt processes have a weaker effect on soil temperature (Zheng et al., 2022). With a relatively warm and humid climate, vegetation growth can better absorb and utilize the snowmelt water as there is no permafrost in the way (Ran et al., 2021) and spring snowmelt can penetrate the soil more quickly (Harpold & Molotch, 2015; Iwata et al., 2010). Therefore, the warmer the area, the stronger the effect of SCED on SOS in these warm areas.

4.3. Limitations

Data acquired from GlobSnow are subject to certain uncertainties in estimating SWE above 150 mm or in forested regions with dense canopy cover (Luojus et al., 2020; Takala et al., 2011). In addition, the lack of GlobSnow data in summer prevents the extraction of SCED in the High Arctic with the long snow season, and therefore our results do not cover the High Arctic region. It also is noted that the NDVI-based SOS based on satellite reflects the average date of the start of ecosystem growth within pixels, which differs from the specific vegetation

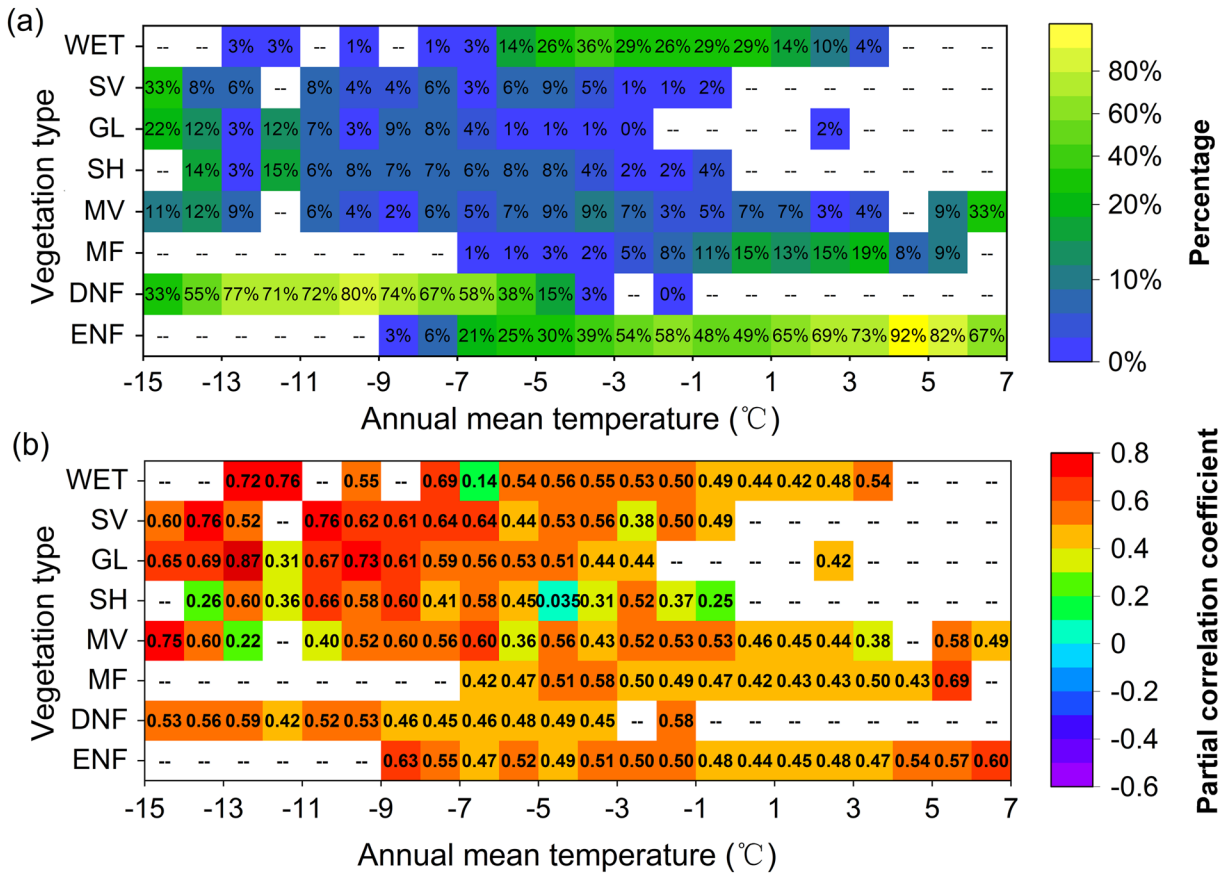

Figure 7. Vegetation differences in the effect of snow cover end date (SCED) on start of the growing season (SOS) under different temperature conditions. (a) is area percentage and (b) is the mean partial correlation coefficient of each vegetation type within each annual mean temperature interval in pixels with the significant partial correlation between SCED and SOS.

phenology observed at ground level by humans (Doktor et al., 2009). In this study, when analyzing the influence of snow cover on the SOS, other factors, such as human activities, nutrients, and frost, are not considered because of insufficient data. Further, although these factors are not major constraints of spring phenological events in present-day climatic conditions, we cannot eliminate the possibility of other variables influencing the changes in vegetation phenology in spring (Ernakovich et al., 2014). Due to the lack of ground observation data, we used only two sites with both available snow depth and vegetation information to somewhat validate the relationship between snow cover and SOS found in our study, as shown in the Supporting Information (Figure S11 and Tables S1, S2). Our current study provides an overall understanding of the effect of snow cover on SOS from the circumpolar scale based on remote sensing data, and further use of higher spatial resolution data as well as long-term in situ observations are needed to study the relations between snow cover and SOS at a finer scale in the future.

4.4. Implication

Future changes projected by global climate models are larger in the Arctic than in the mid-latitudes. Near-surface temperatures continue to rise (Landrum & Holland, 2020) and shrubs may expand in response (Pearson et al., 2013). According to RCP8.5, annual snow cover is projected to decrease by 10%–20% over much of the Arctic by 2055 (AMAP, 2017). Therefore, climate-induced snow cover changes are anticipated to continuously affect vegetation phenology in spring in terrestrial ecosystems. The impact of SCED advancement on spring vegetation phenology is expected to diminish in cold areas and increase in warm areas.

5. Conclusions

This study provides a comprehensive assessment of the impact of snow cover changes on spring vegetation phenology across the Pan-Arctic from a long-term and large-scale perspective. SCED is the main snow indicator

affecting the SOS across the Pan-Arctic, and the SOS is advanced by 0.56 days with SCED advancement by 1 day. In 63% of the Pan-Arctic, SCED can explain 12%–90% of the variation in SOS and is the most important factor influencing SOS in 13% of the Pan-Arctic region. There are significant spatial differences in the influence of SCED on the SOS affected by climatic conditions, which are mainly related to temperature rather than precipitation. The positive effect of SCED on SOS diminished with increasing temperature in cold areas where the mean annual temperature is below 1°C, whereas the positive effect of SCED on SOS increased with increasing temperature in warm areas where the mean annual temperature is above 1°C. This phenomenon may be mainly due to the different functions of snow cover under different vegetation types and climatic conditions.

As warming continues, the impact of early SCED on spring vegetation phenology is expected to diminish in cold areas and increase in warm areas across the Pan-Arctic. These results provide an improved understanding of the impact of snow cover on spring vegetation phenology across the Pan-Arctic and support assessing how future climate change will influence vegetation ecosystems.

Data Availability Statement

All data sets and materials used in this study are freely available online. The GlobSnow SWE data set is downloaded from https://www.globsnow.info/swe/archive_v3.0/. The GIMMS NDVI3g data set is obtained from https://iridl.ldeo.columbia.edu/SOURCES/.NASA/.ARC/.ECOCAST/.GIMMS/.NDVI3g/.v1p0/. The temperature, precipitation, and radiation data are collected from the ECMWF ERA-5 monthly averaged data data set from https://cds.climate.copernicus.eu/cdsapp#!/dataset/reanalysis-era5-single-levels?tab=overview. The CCI LC Land Cover Type Product is downloaded from http://maps.elie.ucl.ac.be/CCI/viewer/download.php. The ground observations of snow depth and vegetation information are available from AmeriFlux (https://ameriflux.lbl.gov/data/download-data/).

Acknowledgments
This study was supported by the National Natural Science Foundation of China (Grant 42171307) and the National Key Research and Development Program of China (Grant 2020YFA0608500).

References

AMAP (2017). *Snow, water, ice and permafrost in the Arctic (SWIPA) 2017* (p. 26). Arctic Monitoring and Assessment Programme (AMAP).

Assmann, J. J., Myers-Smith, I. H., Phillimore, A. B., Bjorkman, A. D., Ennos, R. E., Prevéy, J. S., et al. (2019). Local snow melt and temperature—But not regional sea ice—Explain variation in spring phenology in coastal Arctic tundra. *Global Change Biology*, *25*(7), 2258–2274. https://doi.org/10.1111/gcb.14639

Barrett, A. P., Stroeve, J. C., & Serreze, M. C. (2020). Arctic Ocean precipitation from atmospheric reanalyses and comparisons with North Pole drifting station records. *Journal of Geophysical Research: Oceans*, *125*(1), e2019JC015415. https://doi.org/10.1029/2019JC015415

Bartsch, A., Höfler, A., Kroisleitner, C., & Trofaier, A. M. (2016). Land cover mapping in Northern high latitude permafrost regions with satellite data: Achievements and remaining challenges. *Remote Sensing*, *8*(12), 979. https://doi.org/10.3390/rs8120979

Basler, D., & Körner, C. (2012). Photoperiod sensitivity of bud burst in 14 temperate forest tree species. *Agricultural and Forest Meteorology*, *165*, 73–81. https://doi.org/10.1016/j.agrformet.2012.06.001

Beck, P., Atzberger, C., Høgda, K., Johansen, B., & Skidmore, A. (2006). Improved monitoring of vegetation dynamics at very high latitudes: A new method using MODIS NDVI. *Remote Sensing of Environment*, *100*(3), 321–334. https://doi.org/10.1016/j.rse.2005.10.021

Bjorkman, A. D., Elmendorf, S. C., Beamish, A. L., Vellend, M., & Henry, G. H. R. (2015). Contrasting effects of warming and increased snowfall on Arctic tundra plant phenology over the past two decades. *Global Change Biology*, *21*(12), 4651–4661. https://doi.org/10.1111/gcb.13051

Bokhorst, S., Bjerke, J. W., Street, L. E., Callaghan, T. V., & Phoenix, G. K. (2011). Impacts of multiple extreme winter warming events on sub-arctic heathland: Phenology, reproduction, growth, and CO_2 flux responses. *Global Change Biology*, *17*(9), 2817–2830. https://doi.org/10.1111/j.1365-2486.2011.02424.x

Borner, A. P., Kielland, K., & Walker, M. D. (2008). Effects of simulated climate change on plant phenology and nitrogen mineralization in Alaskan Arctic tundra. *Arctic Antarctic and Alpine Research*, *40*(1), 27–38. https://doi.org/10.1657/1523-0430(06-099)[BORNER]2.0.CO;2

Brown, R., Derksen, C., & Wang, L. (2010). A multi-data set analysis of variability and change in Arctic spring snow cover extent, 1967–2008. *Journal of Geophysical Research*, *115*(D16), D16111. https://doi.org/10.1029/2010JD013975

Buitenwerf, R., Rose, L., & Higgins, S. I. (2015). Three decades of multi-dimensional change in global leaf phenology. *Nature Climate Change*, *5*(4), 364–368. https://doi.org/10.1038/nclimate2533

Buus-Hinkler, J., Hansen, B. U., Tamstorf, M. P., & Pedersen, S. B. (2006). Snow-vegetation relations in a High Arctic ecosystem: Inter-annual variability inferred from new monitoring and modeling concepts. *Remote Sensing of Environment*, *105*(3), 237–247. https://doi.org/10.1016/j.rse.2006.06.016

Cong, N., Wang, T., Nan, H., Ma, Y., Wang, X., Myneni, R. B., & Piao, S. (2013). Changes in satellite-derived spring vegetation green-up date and its linkage to climate in China from 1982 to 2010: A multimethod analysis. *Global Change Biology*, *19*(3), 881–891. https://doi.org/10.1111/gcb.12077

Cooper, E. J., Dullinger, S., & Semenchuk, P. (2011). Late snowmelt delays plant development and results in lower reproductive success in the High Arctic. *Plant Science*, *180*(1), 157–167. https://doi.org/10.1016/j.plantsci.2010.09.005

de Beurs, K. M., & Henebry, G. M. (2005). Land surface phenology and temperature variation in the International Geosphere-Biosphere Program high-latitude transects. *Global Change Biology*, *11*(5), 779–790. https://doi.org/10.1111/j.1365-2486.2005.00949.x

de Beurs, K. M., & Henebry, G. M. (2008). Northern annular mode effects on the land surface phenologies of Northern Eurasia. *Journal of Climate*, *21*(17), 4257–4279. https://doi.org/10.1175/2008JCLI2074.1

de Beurs, K. M., & Henebry, G. M. (2010). A land surface phenology assessment of the northern polar regions using MODIS reflectance time series. *Canadian Journal of Remote Sensing*, *36*(sup1), S87–S110. https://doi.org/10.5589/m10-021

Delbart, N., Le Toan, T., Kergoat, L., & Fedotova, V. (2006). Remote sensing of spring phenology in boreal regions: A free of snow-effect method using NOAA-AVHRR and SPOT-VGT data (1982–2004). *Remote Sensing of Environment*, *101*(1), 52–62. https://doi.org/10.1016/j.rse.2005.11.012

Descals, A., Verger, A., Yin, G., & Peñuelas, J. (2020). Improved estimates of arctic land surface phenology using Sentinel-2 time series. *Remote Sensing*, *12*(22), 3738. https://doi.org/10.3390/rs12223738

Doktor, D., Bondeau, A., Koslowski, D., & Badeck, F.-W. (2009). Influence of heterogeneous landscapes on computed green-up dates based on daily AVHRR NDVI observations. *Remote Sensing of Environment*, *113*(12), 2618–2632. https://doi.org/10.1016/j.rse.2009.07.020

Ernakovich, J. G., Hopping, K. A., Berdanier, A. B., Simpson, R. T., Kachergis, E. J., Steltzer, H., & Wallenstein, M. D. (2014). Predicted responses of arctic and alpine ecosystems to altered seasonality under climate change. *Global Change Biology*, *20*(10), 3256–3269. https://doi.org/10.1111/gcb.12568

ESA. (2017). Land cover CCI product user guide version 2. Tech. Rep. Retrieved from maps.elie.ucl.ac.be/CCI/viewer/download/ESACCI-LC-Ph2-PUGv2_2.0.pdf

Freppaz, M., Celi, L., Marchelli, M., & Zanini, E. (2008). Snow removal and its influence on temperature and N dynamics in alpine soils (Vallee d'Aoste-NW Italy). *Journal of Plant Nutrition and Soil Science*, *171*(5), 672–680. https://doi.org/10.1002/jpln.200700278

Graham, R. M., Hudson, S. R., & Maturilli, M. (2019). Improved performance of ERA5 in Arctic gateway relative to four global atmospheric reanalyses. *Geophysical Research Letters*, *46*(11), 6138–6147. https://doi.org/10.1029/2019GL082781

Groffman, P. M., Driscoll, C. T., Fahey, T. J., Hardy, J. P., Fitzhugh, R. D., & Tierney, G. L. (2001). Colder soils in a warmer world: A snow manipulation study in a northern hardwood forest ecosystem. *Biogeochemistry*, *56*(2), 135–150. https://doi.org/10.1023/A:1013039830323

Hamed, K. H., & Rao, R. A. (1998). A modified Mann-Kendall trend test for autocorrelated data. *Journal of Hydrology*, *204*(1), 182–196. https://doi.org/10.1016/S0022-1694(97)00125-X

Harpold, A. A., & Molotch, N. P. (2015). Sensitivity of soil water availability to changing snowmelt timing in the Western U.S. *Geophysical Research Letters*, *42*(19), 8011–8020. https://doi.org/10.1002/2015GL065855

Hersbach, H., Bell, B., Berrisford, P., Hirahara, S., Horányi, A., Muñoz-Sabater, J., et al. (2020). The ERA5 global reanalysis. *Quarterly Journal of the Royal Meteorological Society*, *146*(730), 1999–2049. https://doi.org/10.1002/qj.3803

Iler, A. M., Inouye, D. W., Schmidt, N. M., & Høye, T. T. (2017). Detrending phenological time series improves climate–phenology analyses and reveals evidence of plasticity. *Ecology*, *98*(3), 647–655. https://doi.org/10.1002/ecy.1690

Iwata, Y., Hayashi, M., Suzuki, S., Hirota, T., & Hasegawa, S. (2010). Effects of snow cover on soil freezing, water movement, and snowmelt infiltration: A paired plot experiment. *Water Resources Research*, *46*(9). https://doi.org/10.1029/2009WR008070

Jiao, W., Wang, L., Smith, W. K., Chang, Q., Wang, H., & D'Odorico, P. (2021). Observed increasing water constraint on vegetation growth over the last three decades. *Nature Communications*, *12*(1), 3777. https://doi.org/10.1038/s41467-021-24016-9

Jin, H., & Eklundh, L. (2014). A physically based vegetation index for improved monitoring of plant phenology. *Remote Sensing of Environment*, *152*, 512–525. https://doi.org/10.1016/j.rse.2014.07.010

Jonas, T., Rixen, C., Sturm, M., & Stoeckli, V. (2008). How alpine plant growth is linked to snow cover and climate variability. *Journal of Geophysical Research*, *113*(G3), G03013. https://doi.org/10.1029/2007JG000680

Keenan, T. F., Gray, J., Friedl, M. A., Toomey, M., Bohrer, G., Hollinger, D. Y., et al. (2014). Net carbon uptake has increased through warming-induced changes in temperate forest phenology. *Nature Climate Change*, *4*(7), 598–604. https://doi.org/10.1038/nclimate2253

Kelsey, K. C., Pedersen, S. H., Leffler, A. J., Sexton, J. O., Feng, M., & Welker, J. M. (2021). Winter snow and spring temperature have differential effects on vegetation phenology and productivity across Arctic plant communities. *Global Change Biology*, *27*(8), 1572–1586. https://doi.org/10.1111/gcb.15505

Kim, J. H., Hwang, T., Yang, Y., Schaaf, C. L., Boose, E., & Munger, J. W. (2018). Warming-induced earlier greenup leads to reduced stream discharge in a temperate mixed forest catchment. *Journal of Geophysical Research: Biogeosciences*, *123*(6), 1960–1975. https://doi.org/10.1029/2018JG004438

Landrum, L., & Holland, M. M. (2020). Extremes become routine in an emerging new Arctic. *Nature Climate Change*, *10*(12), 1108–1115. https://doi.org/10.1038/s41558-020-0892-z

Legault, G., & Cusa, M. (2015). Temperature and delayed snowmelt jointly affect the vegetative and reproductive phenologies of four sub-Arctic plants. *Polar Biology*, *38*(10), 1701–1711. https://doi.org/10.1007/s00300-015-1736-6

Li, L., Liu, Q., Liu, G., Li, H., & Huang, C. (2019). Accuracy evaluation and consistency analysis of four global land cover products in the Arctic region. *Remote Sensing*, *11*(12), 1396. https://doi.org/10.3390/rs11121396

Linderholm, H. W. (2006). Growing season changes in the last century. *Agricultural and Forest Meteorology*, *137*(1), 1–14. https://doi.org/10.1016/j.agrformet.2006.03.006

Lundell, R., Saarinen, T., & Hänninen, H. (2010). Effects of snowmelt on the springtime photosynthesis of the evergreen dwarf shrub Vaccinium vitis-idaea. *Plant Ecology and Diversity*, *3*(2), 121–130. https://doi.org/10.1080/17550874.2010.497195

Luojus, K., Pulliainen, J., Takala, M., Lemmetyinen, J., & Moisander, M. (2020). GlobSnow v3.0 snow water equivalent (SWE) [Dataset]. PANGAEA. https://doi.org/10.1594/PANGAEA.911944

Luus, K. A., Gel, Y., Lin, J. C., Kelly, R. E. J., & Duguay, C. R. (2013). Pan-Arctic linkages between snow accumulation and growing-season air temperature, soil moisture and vegetation. *Biogeosciences*, *10*(11), 7575–7597. https://doi.org/10.5194/bg-10-7575-2013

Meredith, M., Sommerkorn, M., Cassotta, S., Derksen, C., Ekaykin, A., Hollowed, A., et al. (2019). Polar regions. In H.-O. Pörtner, D. C. Roberts, V. Masson-Delmotte, P. Zhai, M. Tignor, E. Poloczanska, et al. (Eds.), *IPCC special report on the ocean and cryosphere in a changing climate* (pp. 203–320). Cambridge University Press. https://doi.org/10.1017/9781009157964.005

Mølgaard, P., & Christensen, K. (2010). Response to experimental warming in a population of papaver radicatum in Greenland. *Global Change Biology*, *3*(S1), 116–124. https://doi.org/10.1111/j.1365-2486.1997.gcb140.x

Mudryk, L. E., Chereque, A., Brown, R., Derksen, C., Luojus, K., & Decharme, B. (2020). Arctic report card 2020: Terrestrial snow cover. https://doi.org/10.25923/p6ca-v923

Myneni, R. B., Hall, F. G., Sellers, P. J., & Marshak, A. L. (1995). The interpretation of spectral vegetation indexes. *IEEE Transactions on Geoscience and Remote Sensing*, *33*(2), 481–486. https://doi.org/10.1109/TGRS.1995.8746029

Oberbauer, S. F., Elmendorf, S. C., Troxler, T. G., Hollister, R. D., Rocha, A. V., Bret-Harte, M. S., et al. (2013). Phenological response of tundra plants to background climate variation tested using the International Tundra Experiment. *Philosophical Transactions of the Royal Society B: Biological Sciences*, *368*(1624), 20120481. https://doi.org/10.1098/rstb.2012.0481

Panchen, Z. A., & Gorelick, R. (2017). Prediction of Arctic plant phenological sensitivity to climate change from historical records. *Ecology and Evolution*, *7*(5), 1325–1338. https://doi.org/10.1002/ece3.2702

Park, H., Jeong, S.-J., Ho, C.-H., Park, C.-E., & Kim, J. (2018). Slowdown of spring green-up advancements in boreal forests. *Remote Sensing of Environment*, *217*, 191–202. https://doi.org/10.1016/j.rse.2018.08.012

Paudel, K., & Andersen, P. (2012). Response of rangeland vegetation to snow cover dynamics in Nepal Trans Himalaya. *Climatic Change*, *117*(1–2), 149–162. https://doi.org/10.1007/s10584-012-0562-x

Pearson, R. G., Phillips, S. J., Loranty, M. M., Beck, P. S. A., Damoulas, T., Knight, S. J., & Goetz, S. J. (2013). Shifts in Arctic vegetation and associated feedbacks under climate change. *Nature Climate Change*, *3*(7), 673–677. https://doi.org/10.1038/nclimate1858

Penuelas, J., Rutishauser, T., & Filella, I. (2009). Phenology feedbacks on climate change. *Science (New York, N.Y.)*, *324*(5929), 887–888. https://doi.org/10.1126/science.1173004

Piao, S., Liu, Q., Chen, A., Janssens, I. A., Fu, Y., Dai, J., et al. (2019). Plant phenology and global climate change: Current progresses and challenges. *Global Change Biology*, *25*(6), 1922–1940. https://doi.org/10.1111/gcb.14619

Pinzon, J. E., & Tucker, C. J. (2014). A non-stationary 1981–2012 AVHRR NDVI3g time series. *Remote Sensing*, *6*(8), 6929–6960. https://doi.org/10.3390/rs6086929

Prevéy, J., Vellend, M., Rüger, N., Hollister, R. D., Bjorkman, A. D., Myers-Smith, I. H., et al. (2017). Greater temperature sensitivity of plant phenology at colder sites: Implications for convergence across northern latitudes. *Global Change Biology*, *23*(7), 2660–2671. https://doi.org/10.1111/gcb.13619

Pulliainen, J. (2006). Mapping of snow water equivalent and snow depth in boreal and sub-arctic zones by assimilating space-borne microwave radiometer data and ground-based observations. *Remote Sensing of Environment*, *101*(2), 257–269. https://doi.org/10.1016/j.rse.2006.01.002

Pulliainen, J., Luojus, K., Derksen, C., Mudryk, L., Lemmetyinen, J., Salminen, M., et al. (2020). Patterns and trends of Northern Hemisphere snow mass from 1980 to 2018. *Nature*, *581*(7808), 294–298. https://doi.org/10.1038/s41586-020-2258-0

Ran, Y., Jorgenson, M. T., Li, X., Jin, H., Wu, T., Li, R., & Cheng, G. (2021). Biophysical permafrost map indicates ecosystem processes dominate permafrost stability in the Northern Hemisphere. *Environmental Research Letters*, *16*(9), 095010. https://doi.org/10.1088/1748-9326/ac20f3

Richardson, A. D., Keenan, T. F., Migliavacca, M., Ryu, Y., Sonnentag, O., & Toomey, M. (2013). Climate change, phenology, and phenological control of vegetation feedbacks to the climate system. *Agricultural and Forest Meteorology*, *169*, 156–173. https://doi.org/10.1016/j.agrformet.2012.09.012

Rixen, C., Freppaz, M., Stoeckli, V., Huovinen, C., Huovinen, K., & Wipf, S. (2008). Altered snow density and chemistry change soil nitrogen mineralization and plant growth. *Arctic Antarctic and Alpine Research*, *40*(3), 568–575. https://doi.org/10.1657/1523-0430(07-044)[RIXEN]2.0.CO;2

Semenchuk, P. R., Gillespie, M. A. K., Rumpf, S. B., Baggesen, N., Elberling, B., & Cooper, E. J. (2016). High arctic plant phenology is determined by snowmelt patterns but duration of phenological periods is fixed: An example of periodicity. *Environmental Research Letters*, *11*(12), 125006. https://doi.org/10.1088/1748-9326/11/12/125006

Shen, M., Zhang, G., Cong, N., Wang, S., Kong, W., & Piao, S. (2014). Increasing altitudinal gradient of spring vegetation phenology during the last decade on the Qinghai–Tibetan Plateau. *Agricultural and Forest Meteorology*, *189*, 71–80. *–190*. https://doi.org/10.1016/j.agrformet.2014.01.003

Sherwood, J. A., Debinski, D. M., Caragea, P. C., & Germino, M. J. (2017). Effects of experimentally reduced snowpack and passive warming on montane meadow plant phenology and floral resources. *Ecosphere*, *8*(3), e01745. https://doi.org/10.1002/ecs2.1745

Shimono, Y., & Kudo, G. (2005). Comparisons of germination traits of alpine plants between fellfield and snowbed habitats. *Ecological Research*, *20*(2), 189–197. https://doi.org/10.1007/s11284-004-0031-8

Takala, M., Luojus, K., Pulliainen, J., Derksen, C., Lemmetyinen, J., Kärnä, J.-P., et al. (2011). Estimating northern hemisphere snow water equivalent for climate research through assimilation of space-borne radiometer data and ground-based measurements. *Remote Sensing of Environment*, *115*(12), 3517–3529. https://doi.org/10.1016/j.rse.2011.08.014

Tian, F., Fensholt, R., Verbesselt, J., Grogan, K., Horion, S., & Wang, Y. (2015). Evaluating temporal consistency of long-term global NDVI datasets for trend analysis. *Remote Sensing of Environment*, *163*, 326–340. https://doi.org/10.1016/j.rse.2015.03.031

Totland, O., & Alatalo, J. M. (2002). Effects of temperature and date of snowmelt on growth, reproduction, and flowering phenology in the arctic/alpine herb, Ranunculus glacialis. *Oecologia*, *133*(2), 168–175. https://doi.org/10.1007/s00442-002-1028-z

Trolliet, M., Walawender, J. P., Bourlès, B., Boilley, A., Trentmann, J., Blanc, P., et al. (2018). Downwelling surface solar irradiance in the tropical Atlantic Ocean: A comparison of re-analyses and satellite-derived data sets to PIRATA measurements. *Ocean Science*, *14*(5), 1021–1056. https://doi.org/10.5194/os-14-1021-2018

Walther, G. R., Beissner, S., & Burga, C. A. (2005). Trends in the upward shift of alpine plants. *Journal of Vegetation Science*, *16*(5), 541–548. https://doi.org/10.1111/j.1654-1103.2005.tb02394.x

Wang, J., Liu, D., Ciais, P., & Peñuelas, J. (2022). Decreasing rainfall frequency contributes to earlier leaf onset in northern ecosystems. *Nature Climate Change*, *12*(4), 386–392. https://doi.org/10.1038/s41558-022-01285-w

Wang, K., Zhang, L., Qiu, Y., Ji, L., Tian, F., Wang, C., & Wang, Z. (2015). Snow effects on alpine vegetation in the Qinghai-Tibetan Plateau. *International Journal of Digital Earth*, *8*(1), 58–75. https://doi.org/10.1080/17538947.2013.848946

Wang, S., Wang, X., Chen, G., Yang, Q., Wang, B., Ma, Y., & Shen, M. (2017). Complex responses of spring alpine vegetation phenology to snow cover dynamics over the Tibetan Plateau, China. *Science of the Total Environment*, *593–594*, 449–461. https://doi.org/10.1016/j.scitotenv.2017.03.187

Wang, X., Piao, S., Ciais, P., Li, J., Friedlingstein, P., Koven, C., & Chen, A. (2011). Spring temperature change and its implication in the change of vegetation growth in North America from 1982 to 2006. *Proceedings of the National Academy of Sciences*, *108*(4), 1240–1245. https://doi.org/10.1073/pnas.1014425108

Wang, X., Wang, T., Guo, H., Liu, D., Zhao, Y., Zhang, T., et al. (2017). Disentangling the mechanisms behind winter snow impact on vegetation activity in northern ecosystems. *Global Change Biology*, *24*(4), 1651–1662. https://doi.org/10.1111/gcb.13930

Wang, X., Wu, C., Peng, D., Gonsamo, A., & Liu, Z. (2018). Snow cover phenology affects alpine vegetation growth dynamics on the Tibetan Plateau: Satellite observed evidence, impacts of different biomes, and climate drivers. *Agricultural and Forest Meteorology*, *256–257*, 61–74. https://doi.org/10.1016/j.agrformet.2018.03.004

Wang, X., Xiao, J., Li, X., Cheng, G., Ma, M., Zhu, G., et al. (2019). No trends in spring and autumn phenology during the global warming hiatus. *Nature Communications*, *10*(1), 2389. https://doi.org/10.1038/s41467-019-10235-8

Weintraub, M., & Schimel, J. (2003). Interactions between carbon and nitrogen mineralization and soil organic matter chemistry in Arctic tundra soils. *Ecosystems*, *6*(2), 0129–0143. https://doi.org/10.1007/s10021-002-0124-6

Westergaard-Nielsen, A., Lund, M., Pedersen, S. H., Schmidt, N. M., Klosterman, S., Abermann, J., & Hansen, B. U. (2017). Transitions in high-Arctic vegetation growth patterns and ecosystem productivity tracked with automated cameras from 2000 to 2013. *Ambio*, *46*(1), 39–52. https://doi.org/10.1007/s13280-016-0864-8

Wheeler, H. C., Høye, T. T., Schmidt, N. M., Svenning, J.-C., & Forchhammer, M. C. (2015). Phenological mismatch with abiotic conditions—Implications for flowering in Arctic plants. *Ecology*, *96*(3), 775–787. https://doi.org/10.1890/14-0338.1

White, M. A., Thornton, P. E., & Running, S. W. (1997). A continental phenology model for monitoring vegetation responses to interannual climatic variability. *Global Biogeochemical Cycles*, *11*(2), 217–234. https://doi.org/10.1029/97GB00330

Wipf, S. (2010). Phenology, growth, and fecundity of eight subarctic tundra species in response to snowmelt manipulations. *Plant Ecology*, *207*(1), 53–66. https://doi.org/10.1007/s11258-009-9653-9

Wipf, S., & Rixen, C. (2010). A review of snow manipulation experiments in Arctic and alpine tundra ecosystems. *Polar Research*, *29*(1), 95–109. https://doi.org/10.1111/j.1751-8369.2010.00153.x

Wipf, S., Rixen, C., & Mulder, C. P. H. (2006). Advanced snowmelt causes shift towards positive neighbour interactions in a subarctic tundra community. *Global Change Biology*, *12*(8), 1496–1506. https://doi.org/10.1111/j.1365-2486.2006.01185.x

Wu, C., Gonsamo, A., Gough, C. M., Chen, J. M., & Xu, S. (2014). Modeling growing season phenology in North American forests using seasonal mean vegetation indices from MODIS. *Remote Sensing of Environment*, *147*, 79–88. https://doi.org/10.1016/j.rse.2014.03.001

Wu, C., Wang, J., Ciais, P., Peñuelas, J., Zhang, X., Sonnentag, O., et al. (2021). Widespread decline in winds delayed autumn foliar senescence over high latitudes. *Proceedings of the National Academy of Sciences*, *118*(16), e2015821118. https://doi.org/10.1073/pnas.2015821118

Xie, J., Kneubühler, M., Garonna, I., Jong, R. D., Notarnicola, C., Gregorio, L. D., & Schaepman, M. E. (2018). Relative influence of Timing and accumulation of snow on alpine land surface phenology. *Journal of Geophysical Research: Biogeosciences*, *123*(2), 561–576. https://doi.org/10.1002/2017JG004099

Yu, Z., Liu, S., Wang, J., Sun, P., Liu, W., & Hartley, D. S. (2013). Effects of seasonal snow on the growing season of temperate vegetation in China. *Global Change Biology*, *19*(7), 2182–2195. https://doi.org/10.1111/gcb.12206

Zeng, H., Jia, G., & Epstein, H. (2011). Recent changes in phenology over the northern high latitudes detected from multi-satellite data. *Environmental Research Letters*, *6*(4), 045508. https://doi.org/10.1088/1748-9326/6/4/045508

Zeng, L., Wardlow, B. D., Xiang, D., Hu, S., & Li, D. (2020). A review of vegetation phenological metrics extraction using time-series, multispectral satellite data. *Remote Sensing of Environment*, *237*, 111511. https://doi.org/10.1016/j.rse.2019.111511

Zheng, J., Jia, G., & Xu, X. (2022). Earlier snowmelt predominates advanced spring vegetation greenup in Alaska. *Agricultural and Forest Meteorology*, *315*, 108828. https://doi.org/10.1016/j.agrformet.2022.108828

Zheng, J., Xu, X., Jia, G., & Wu, W. (2020). Understanding the spring phenology of Arctic tundra using multiple satellite data products and ground observations. *Science China Earth Sciences*, *63*(10), 1599–1612. https://doi.org/10.1007/s11430-019-9644-8

Zhong, X., Zhang, T., Kang, S., & Wang, J. (2021). Spatiotemporal variability of snow cover timing and duration over the Eurasian continent during 1966–2012. *Science of the Total Environment*, *750*, 141670. https://doi.org/10.1016/j.scitotenv.2020.141670

References From the Supporting Information

Euskirchen, E. (2021). AmeriFlux US-BZB Bonanza Creek Thermokarst Bog, version 1-5. [Dataset]. AmeriFlux AMP. https://doi.org/10.17190/AMF/1773401

Euskirchen, E., Shaver, G., & Bret-Harte, S. (2016). AmeriFlux US-ICh Imnavait Creek Watershed Heath Tundra, version 2-1. [Dataset]. AmeriFlux AMP. https://doi.org/10.17190/AMF/1246133